

**CALCULATION OF THE FISSION Q-VALUE
AND SPATIAL ENERGY DEPOSITION IN THE
SAFARI-1 NUCLEAR REACTOR**

Linina Jurbandam

A Dissertation submitted to the Faculty of Science,
University of the Witwatersrand, in fulfilment of
the requirements for the degree of
Master of Science.

Johannesburg, 2018.

DECLARATION

I, Linina Jurbandam, declare that this Dissertation is my own, unaided work. It is being submitted for the Degree of Master of Science at the University of the Witwatersrand, Johannesburg. It has not been submitted before for any degree or examination at any other university.

Linina Jurbandam

30th day of October 2018 at Johannesburg.

ABSTRACT

The calculation of reactor-specific fission Q-values is important for the safety analyses of nuclear reactors. The recoverable energy from the fission Q-value is used to normalise reactor quantities to the total power of the reactor. In this work, a detailed recoverable energy from fission Q-value and spatial heat deposition calculations are presented for the SAFARI-1 nuclear reactor. The fission Q-value is composed of the energy released in a fission event by fission products, neutrons, prompt and delayed gamma rays, beta particles and neutrinos. The energy released by neutrinos is not recoverable; however, part of it is recovered by the gamma and beta radiation from the decay of activated materials. We present two methods to calculate the recoverable energy released per fission. The first one uses the Monte Carlo N-Particle (MCNP5) code. MCNP is a probabilistic transport code that has the capability of calculating most of the heating contributions due to particle interactions with matter. The second method uses the Evaluated Nuclear Data File, ENDF/B-VII and ENDF/B-VII.1 data libraries. The ENDF data libraries contains the information required to calculate all the fission Q-value components, except the energy released from radiative capture, since this quantity depends on the reactor materials. To calculate this, we use the radiative capture reaction rate in MCNP5 and the binding energy of the product of the activation. We obtained a final Q-value of 200.8 ± 0.6 MeV/fission for SAFARI-1. Using the fission Q-value result, we obtained the spatial heat distribution for SAFARI-1 by

calculating the heating rates of the Q-value components. It was established that 97% of the heat produced is deposited in the fuel and 3% is deposited in the surrounding region of the reactor.

DEDICATION

I dedicate this work to my loving mum and dad who have supported me through all my endeavours in life. Thank you mum, and dad, and may you both rest in peace.

ACKNOWLEDGEMENTS

First and foremost, I thank God Almighty for giving me the strength to complete this work during an emotional and difficult two years of my life. I express my sincere gratitude to my supervisor and mentor, Dr. Oscar Zamonsky. Thank you to all the Radiation and Reactor theory staff members at Necsa for supporting me in this endeavour. A special thank you to Hantie Labuschagne for motivating me every day during every battle that I have faced. I would like to thank Dr. Iyabo Usman for all her patience and understanding during my studies. I would also like to express my special gratitude to Dr. Lindsay Donaldson who has not only been a mentor to me during my studies, but has also been a close friend to me during extremely difficult times in my life. I wish to express my sincere thanks to my family who have supported me endlessly throughout this endeavour. Thank you, Nashvir, for being my pillar of strength.

Lastly, I would like to thank the National Research Foundation, Necsa and the University of the Witwatersrand for funding me during my studies.

CONTENTS

DECLARATION	i
ABSTRACT	ii
DEDICATION	iv
ACKNOWLEDGEMENTS	v
LIST OF FIGURES	xi
LIST OF TABLES	xi
LIST OF ABBREVIATIONS	xii
1 INTRODUCTION	1
2 THEORETICAL BACKGROUND	5
2.1 Neutron Transport	6
2.1.1 Introduction to Concepts in Neutron Transport	6
2.1.1.1 Neutron Cross Sections	7

2.1.1.2	Some Important Quantities of Neutron Physics	9
2.2	The Boltzmann Transport Equation	12
2.3	Deterministic and Probabilistic Methods	14
2.4	Q-Value Energy Components	15
2.5	Spatial Heat Distribution in Reactor Components	17
2.6	Description of the SAFARI-1 Nuclear Reactor	18
2.7	SAFARI-1 Analysis Codes: OSCAR-4 and MCNP5	19
2.8	MCNP Model of SAFARI-1	22
2.8.1	Heating Tallies in MCNP	24
2.8.1.1	The F6 Heating Tally	25
2.8.1.2	The F7 Heating Tally	26
2.9	ENDF/B-VII and ENDF/B-VII.1 Data Libraries	27
3	NUMERICAL EXPERIMENTS AND DATA EXTRACTION	28
3.1	Fission Q-Value Calculation Using MCNP5	29
3.1.1	Procedure to Calculate the Q-value with MCNP5	29
3.2	Calculation of Energy Deposited from Radiative Capture ($Q_{\gamma c}$) Using MCNP5	31
3.2.1	Description of the Radiative Capture Reaction Rate in MCNP	32
3.2.2	Calculation of $Q_{\gamma c}$ using the Radiative Capture Reaction Rate	33
3.3	Calculation of Fission Q-Value Components Using ENDF/B-VII and ENDF/B-VII.1	35
3.3.1	Calculation of Q-value Components using ENDF/B-VII Equations	36

3.3.2	Calculation of Q-value Components using ENDF/B-VII.1	38
3.4	Spatial Heat Distribution in SAFARI-1	40
3.4.1	Calculation of the Spatial Heat Distribution Due to Prompt Energy Components	40
3.4.2	Calculation of the Spatial Heat Distribution due to Fission Product Decay	41
4	RESULTS AND DISCUSSION	44
4.1	Q-Value Results Using MCNP5	46
4.2	Calculation of $Q_{\gamma c}$ by the Activation of the Reactor Components	48
4.3	Q-Value Results Obtained Using ENDF/B-VII and ENDF/B-VII.1	49
4.4	Comparison of Q-Values at Different Stages in a Cycle	52
4.5	Results Obtained for the Spatial Heat Distribution in SAFARI-1	53
5	CONCLUSIONS	56
5.1	Future Work	57
	REFERENCES	57
	APPENDIX A	61
A	MCNP: EXPLANATION OF INPUT AND OUTPUT	61
A.1	MCNP Input	61
A.2	MCNP Output	62

LIST OF FIGURES

2.1	The Important variables used in the Neutron Transport Equation	10
2.2	Reduced decay scheme of Al-28 [1]	12
2.3	The MCNP SAFARI-1 core configuration	23
2.4	Planar view of fuel element with 19 plates, and the absorbing and follower region of the control rod respectively	24
A.1	Example of statistics check from MCNP output	65

LIST OF TABLES

2.1	Emitted and recoverable fission energy components of U-235 [MeV/fission] [2]	16
2.2	Spatial heat distribution of U-235 and Pu-239 [MeV/fission]	17
3.1	List of elements present in the SAFARI-1 reactor core	33
3.2	Binding energies of the nuclides present in SAFARI-1 [3]	34
3.3	Decay energies of unstable nuclei in SAFARI-1	35
3.4	Madland's recommended energy release polynomial coefficients [MeV]	39
4.1	Q-value results obtained using MCNP5 and ENDF/B-VII [MeV/fission]	47
4.2	The Q-value result obtained for radiative capture ($Q_{\gamma c}$) and activation heating from beta decay [MeV/fission]	48
4.4	Fission reaction rate of fuel nuclides in SAFARI-1	49
4.3	Q-value components of fission obtained using the ENDF/B data libraries for various nuclides [MeV/fission]	50
4.5	Weighted averages of U-235/U-238/Pu-239 [MeV/fission]	51
4.6	Q-value results obtained for ENDF/B [MeV/fission]	51

4.7	Comparison of Q-values for different stages in a typical SAFARI-1 cycle [MeV/fission]	52
4.8	Energy deposition in different components of SAFARI-1 [MW] . .	54

LIST OF ABBREVIATIONS

MCNP	Monte Carlo N-Particle
ENDF	Evaluated Nuclear Data File
BOC	Beginning-Of-Cycle
EOC	End-Of-Cycle
FRR	Fission Reaction Rate
RCRR	Radiative Capture Reaction Rate
RRT	Radiation and Reactor Theory
Necsa	South African Nuclear Energy Corporation SOC Ltd
OSCAR	Overall System for the Calculation of Reactors
MTR	Material Testing Reactor
HFIR	High Flux Isotope Reactor
ATR	Advanced Test Reactor
VHTR	Very High Temperature Reactor
FOM	Figure of Merit
PDF	Probability Density Function
IRP	Irradiation Rig Position
PIKMT	Photon-production bias card for coupled neutron-photon problems
SD card	Segment Divider card
SCRAM	Safety Control Rod Axe Man

CHAPTER 1

INTRODUCTION

“Begin at the beginning," the King said, very gravely, "and go on till you come to the end: then stop.” — Lewis Carrol, Alice in Wonderland

Safety forms a crucial part of successful reactor operations. One of the important quantities that are used in safety analyses of the reactor is the fission Q-value which, in particular, is used to normalise neutron fluxes and reaction rates to the operating power of the reactor. The calculation of the fission Q-value can be somewhat complex, because it requires the simulation of radiation particles. Radiation particles deposits energy in the reactor during particle transport. Particle transport can be modelled using probabilistic and deterministic methods. This work focuses on probabilistic methods. Radiation particles released in fission, follow a “random behaviour”, based on an order of probabilistic events. Another important piece of knowledge for reactor safety is the spatial heat energy distribution in the reactor. Nuclear fission results in the release of gamma and beta radiation, fission products and neutrons. The energy released in fission is distributed throughout the reactor. For this work, the MCNP5 transport code was used [4].

The main benefit of MCNP is that it enables the user to perform coupled neutron and photon transport in the reactor, using continuous energy cross section data, and generalised geometries. The continuous energy data are present in nuclear data libraries. There are several nuclear data libraries that can be used. For this work in particular, the Evaluated Nuclear Data File (ENDF) data libraries were used.

The primary goal of this work is to calculate the reactor-specific Q-value for the South African Fundamental Atomic Research Installation 1 (SAFARI-1) nuclear reactor, located at the South African Nuclear Energy Corporation (Necsa) in Pelindaba, South Africa. With the knowledge of the reactor specific Q-value, our next goal is to calculate the spatial heat distribution in SAFARI-1. The spatial heat distribution is important for the safe operation of the reactor because scientists and engineers require the percentage distribution of heat in the reactor core and the surrounding region of the reactor. In this work, a procedure that can be used to calculate the Q-value and spatial heat distribution in any reactor configuration is documented. In addition, the calculations of these quantities for SAFARI-1 are presented. The Q-value that we calculate in this work is an estimate of the total energy released per fission event in SAFARI-1.

The fission Q-value comprises prompt kinetic energy and decay energy from fission product decay. The prompt kinetic energy is due to fission products (Q_{fp}), prompt and delayed neutrons (Q_n), prompt gamma rays ($Q_{\gamma p}$) and neutrinos. During fission product decay, energy is released in the form of beta rays (Q_{β}) and delayed gamma rays ($Q_{\gamma d}$). All the energy released in fission can be recovered in the reactor except for the energy due to neutrinos. Part of this energy, however, can be recovered through the radiative capture that occurs in core materials ($Q_{\gamma c}$). In general, radiative capture can range between 3 - 12 MeV/fission, and the energy lost to neutrinos is 12 MeV/fission [2]. Q-values of reactors range between

198 - 207 MeV/fission [2]. In this range, in thermal reactors, fission fragments account for most of the recoverable energy - approximately 168 MeV/fission. Approximately 15 MeV/fission is recoverable from fission product decay, and around 5 MeV/fission and 7 MeV/fission can be recovered from neutrons and prompt gammas, respectively [2]. The contribution that accounts for variation in the Q-value between different reactors is the energy released from radiative capture. Radiative capture strongly depends on the materials present in the reactor, and therefore, we cannot approximate this value from data libraries. The mixture of fissionable actinides in the core might also affect the Q-value. In SAFARI-1, the majority of the fission reactions during a cycle are due to U-235. This was verified by calculating the fission reaction rate of U-235, U-238 and Pu-239 in SAFARI-1 (Table 3.15).

In this work, two methods of calculating the reactor-specific Q-value for SAFARI-1 are presented. The first method is based on MCNP5 calculations. We use MCNP5 to perform a global heat calculation of the entire reactor. Using the MCNP results, the methodology from reference [5] is followed to calculate the final Q-value. MCNP cannot calculate the heat contribution from fission product decay, therefore, ENDF/B-VII will be used to calculate these contributions. The Q-value is calculated at the beginning-of-cycle (BOC) and the end-of-cycle (EOC) in order to study the effect of burn-up on it.

The second method uses the ENDF/B-VII and ENDF/B-VII.1 libraries to calculate the Q-value. The data in these libraries depends on the energy of the incident neutrons producing fission (E_n). This value was calculated for SAFARI-1, and is given in Chapter 4. The ENDF libraries do not contain information to calculate radiative capture. An independent method is, therefore, performed to calculate it by using the radiative capture reaction rate in MCNP5.

Once the Q-value of SAFARI-1 is known, a spatial heat calculation is performed using heating rates of Q-value components and the heating tallies in MCNP5. We then calculate the percentage spatial heat distribution in the fuel and the surrounding region of the reactor.

The Q-value for SAFARI-1 was calculated to be 200.8 MeV/fission. Similar studies done for the High flux Isotope Reactor (HFIR) reactor yielded 200.2 MeV for BOC and 201.3 MeV for EOC [5]. For the Advanced Test Reactor (ATR) BOC, the Q-value was calculated as 201.4 MeV [5], [6], and for the Very high Temperature Reactor (VHTR), the Q-value varies between 199.6 - 201.6 MeV [7, 8]. This dissertation can be used as a reference for similar types of calculations.

CHAPTER 2

THEORETICAL BACKGROUND

“Before I came here I was confused about this subject. Having listened to your lecture I am still confused. But on a higher level.” — Enrico Fermi

The safety of the environment and personnel working in a reactor environment is of utmost importance. The major concern in any nuclear reactor environment is the radiation produced from nuclear processes. Although the reactor is contained within several layers of material shielding, the radiation particles interact with matter and energy is released in these interactions.

Chapter 2 focuses on the theoretical background required, in order to follow the logic in the subsequent chapters. Firstly, an introduction to neutron transport is given with the Boltzmann transport equation. The Q-value components are then given together with some values that have been measured in literature. The next part of the chapter is a brief description of SAFARI-1 and a detailed description of the MCNP model of SAFARI-1. We also look at the support codes that are used for reactor core analysis. In particular, we focus on MCNP5 since it was used to aid us in most of the calculations for this work. MCNP version 5.1.51 [4]

was used. We take a look at how MCNP can be used to assist in the calculation of the reactor-specific Q-value and spatial heating in SAFARI-1. The last part of the chapter focuses on how we can utilize the ENDF data libraries to calculate the Q-value.

2.1 Neutron Transport

In reactor theory, it is important to know the neutron distribution in the reactor, because it determines the rate at which different nuclear reactions take place. A thorough understanding of neutron transport is imperative when determining the neutron distribution. It is the motion of neutrons in the reactor that eventually leads to scattering, absorption or leakage.

The knowledge of the neutron and gamma distribution in the reactor, and reactor power distribution from neutron population is important for the core design of the reactor. Other important applications of neutron transport analysis in reactors include: radiation-shielding design, heating calculations and also nuclear-plant life, which is determined by the amount of damage done to the reactor pressure vessel as a result of radiation heating.

In this section, an introduction to the Boltzmann transport equation will be given, together with the reactor-physics concepts that are needed to understand the equation.

2.1.1 Introduction to Concepts in Neutron Transport

Neutrons are emitted from a source and continue to stream in a straight line for some distance at which point they leak out of the system or collide and interact with matter. On collision, scattering or absorption may occur. There are two

types of scattering phenomena that may occur. The first type is elastic scattering (n, n) , and the second is inelastic scattering (n, n') . In absorption, there are also two possibilities of reactions that may occur. The first is capture reactions, denoted by: $((n, \gamma), (n, p), (n, \alpha), (n, 2n), (n, 3n))$, and the second is fission reactions, denoted by (n, f) . For this work in particular, our interest lies in absorption of neutrons which is capture and fission. The nuclear cross sections that we use for this work quantifies the probability of neutrons interacting with a material. There are two types of neutron cross sections, macroscopic cross sections and microscopic cross sections.

2.1.1.1 Neutron Cross Sections

The macroscopic cross section is the probability of neutron interaction per unit length. Consider a mono-energetic and uni-dimensional beam of neutrons with intensity $I_0[\frac{\text{neutrons}}{\text{cm}^2 \cdot \text{second}}]$ that is incident on a perpendicular plate of width x . The thickness of the plate is small enough such that the neutron beam will only deviate from its original direction upon a single collision with the plate [2]. Under these conditions, it is observed that the intensity of neutrons that pass through the plate without interaction I_x , is given by:

$$I_x = I_0 e^{-\Sigma_t x}. \quad (2.1)$$

Σ_t is called the macroscopic total cross section of the material of the plate, and its units are cm^{-1} . This quantity depends on the density and composition of the material, as well as the energy of the incident neutrons.

From the previous observations, it follows that the probability, denoted by $p_{ni}(x)$, of having an interaction in an interval Δx , is given by:

$$p_{ni}(x) = \frac{I(x) - I(x + \Delta x)}{I(x)} = 1 - e^{-\sum_t \Delta x}, \quad (2.2)$$

where $p_{ni}(x) \rightarrow \sum_t \Delta x$, when $\Delta x \rightarrow 0$. This means that \sum_t is the probability of having an interaction per unit length.

The probability of crossing the distance x without interacting with the medium is then given by:

$$\frac{I(x)}{I_0} = e^{-\sum_t x}. \quad (2.3)$$

Each reaction type is characterized by its cross section, and the sub-index after \sum usually refers to the type of reaction. Some examples are as follows:

\sum_s is the probability of having a scattering reaction per unit length, \sum_a is the probability of having an absorption reaction per unit length, etc.

In general,

$$\sum = \sum_c + \sum_f + \sum_{n,2n}, \quad (2.4)$$

and

$$\sum = \sum_c + \sum_{n,\gamma} + \sum_{n,p} + \sum_{n,\alpha}, \quad (2.5)$$

where \sum_a , \sum_c , and \sum_f are the absorption, capture and fission cross sections respectively.

When there is no interference in the target nucleus, it has been verified that $\sum_x = N\sigma_x$, where N is the atomic density of the media [at.cm^{-3}], and σ_x is the microscopic cross section of the target material for reaction x . The magnitude of σ is approximately 10^{-24}cm^2 , which is equivalent to 1 barn - the standard unit of

measurement.

The probability per unit path for a neutron to interact with a mix of nuclei $i = 1 \dots N$ is equal to the sum of the individual probabilities,

$$\Sigma = \sum_i N_i \sigma_i. \quad (2.6)$$

For example, in water with density ρ , $\sigma(H)$ and $\sigma(O)$ are the microscopic cross sections of hydrogen and oxygen respectively, then:

$$A(H_2O) = 2A(H) + A(O), \quad N_H = \frac{2N_A \rho}{A(H_2O)} \quad \text{and} \quad N_O = \frac{N_A \rho}{A(H_2O)},$$

where,

A is the atomic number, and N_A is Avagadro's Number.

The same applies to isotopic compositions. If we consider UO_2 , where U is natural uranium, then

$$\Sigma(UO_2) = N_O \times \sigma_O + 0.007N_U \sigma(U_5) + 0.993N_U \sigma(U_8).$$

2.1.1.2 Some Important Quantities of Neutron Physics

Reference [9] was used to explain the theory in this section.

The important variables used in the neutron transport equation are as follows: \vec{r} represents space (x,y,z), $\hat{\Omega} = \hat{\Omega}(\theta, \varphi)$ represents direction, E represents energy, and lastly t is a representation of time. Figure 2.1 represents a point in phase space denoted by $\mathbf{p} = (\vec{r}, \hat{\Omega}, E, t)$.

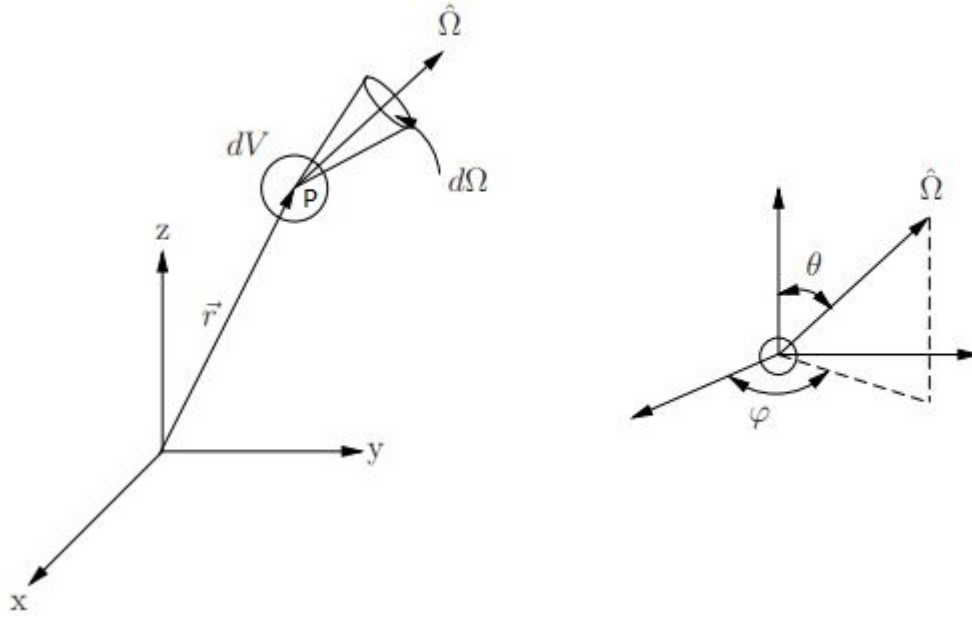


Figure 2.1: The Important variables used in the Neutron Transport Equation

The angular neutron density is defined by N . This should not be confused with the previous definition of N used to represent the sum of probabilities. The angular neutron density is given by:

$$N(\vec{r}, \hat{\Omega}, E, t) dV d\Omega dE$$

which denotes the expected number of neutrons in a volume element dV located at \vec{r} , travelling in a cone $d\Omega$ about direction $\hat{\Omega}$, with an energy E between E and $E + dE$, at time t . The units of N are $[\text{n.cm}^{-3}.\text{sr}^{-1}.\text{MeV}^{-1}]$.

The angular neutron flux is given by:

$$\psi(\vec{r}, \hat{\Omega}, E, t) = vN(\vec{r}, \hat{\Omega}, E, t), \quad (2.7)$$

where $v = \sqrt{2E/m}$ is the neutron speed in units of $[\text{cm.s}^{-1}]$ and the units of the angular neutron flux are therefore $[\text{n.cm}^{-2}.\text{sr}^{-1}.\text{MeV}^{-1}.\text{s}^{-1}]$.

The scalar neutron flux is given by the integral of the angular flux over all angles:

$$\phi(\vec{r}, E, t) = \int_{4\pi} \psi(\vec{r}, \hat{\Omega}, E, t) d\Omega. \quad (2.8)$$

The units are $[\text{n.cm}^{-2}.\text{MeV}^{-1}.\text{s}^{-1}]$. The scalar flux is used to calculate the neutron reaction rate RR , which is the number of reactions that occur per unit time:

$$RR(t) = \int_E \int_V \Sigma_t(E) \phi(\vec{r}, E, t) dV dE. \quad (2.9)$$

The sources of heat production in a reactor are nuclear fission and radiative capture. Fission, which is an absorption reaction denoted by (n, f) , occurs when a thermal neutron is incident on a fissionable nucleus causing it to split into fission fragments. Fission releases energy in the form of kinetic energy taken from prompt gammas, neutrons and fission products. The fission products decay via beta and gamma emission also depositing their energy in the reactor.

Radiative capture (n, γ) occurs when a nucleus captures a neutron and forms a compound nucleus. The excited compound nucleus decays through the emission of gamma radiation. After this, some nuclides might still be unstable and decay further, emitting delayed beta and gamma radiation. Figure 2.2 illustrates this phenomenon for Al-28. Al-27 captures a neutron and becomes Al-28. Al-28 is unstable and will decay to Si-28 via beta minus decay.

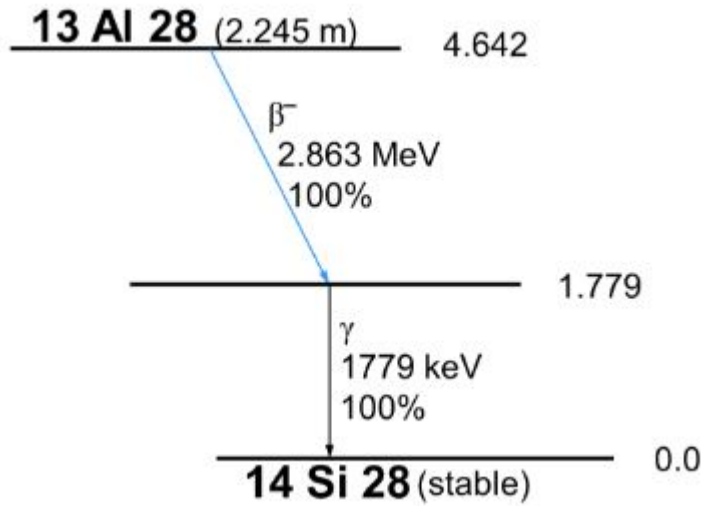


Figure 2.2: Reduced decay scheme of Al-28 [1]

2.2 The Boltzmann Transport Equation

The following assumptions are made in neutron transport theory [10]:

1. Particles are considered as points.
2. Particles travel in straight lines between collisions.
3. Neutron–neutron interactions are neglected.
4. Collisions are considered instantaneous.
5. Material properties are assumed to be isotropic.
6. Nuclear and material properties of the medium are known; and
7. Only the expected mean value of the particle density is considered.

The Boltzmann transport equation is a balanced equation that can be constructed from the following terms.

The rate at which neutrons in $d^3 \vec{r}'$ around \vec{r}' are scattered in the energy interval $[E, dE]$ with directions in $[\hat{\Omega}, d\hat{\Omega}]$ is given by:

$$\left\{ \int_0^\infty dE' \int_{4\pi} d\Omega' \left[\Sigma_s(\vec{r}, \hat{\Omega}' \rightarrow \hat{\Omega}, E' \rightarrow E, t) \psi(\vec{r}, \hat{\Omega}, E) \right] \right\} dE d\hat{\Omega} d^3 \vec{r}', \quad (2.10)$$

and the production in the same interval due to fission can be expressed as:

$$\left\{ \nu \chi(E) \int_0^\infty dE' \Sigma_f(\vec{r}, E') \int_{4\pi} d\Omega' \left[\psi(\vec{r}, \hat{\Omega}', E') \right] \right\} dE d\hat{\Omega} d^3 \vec{r}'. \quad (2.11)$$

The neutron losses in $d^3 \vec{r}'$ around \vec{r}' , $d\hat{\Omega}$ around $\hat{\Omega}$ and dE around E are given by:

$$\left\{ \left[\hat{\Omega} \cdot \vec{\nabla} + \Sigma_t(\vec{r}, E) \right] \psi(\vec{r}, \hat{\Omega}, E) \right\} dE d\hat{\Omega} d^3 \vec{r}', \quad (2.12)$$

and therefore, the transport equation can be written as:

$$\begin{aligned} \frac{1}{v} \frac{\delta \psi(\vec{r}, \hat{\Omega}, E, t)}{\delta t} + \left[\hat{\Omega} \cdot \vec{\nabla} + \Sigma_t(\vec{r}, E) \right] \psi(\vec{r}, \hat{\Omega}, E, t) = \\ \int_0^\infty dE' \int_{4\pi} d\Omega' \left[\Sigma_s(\vec{r}, \hat{\Omega}' \rightarrow \hat{\Omega}, E' \rightarrow E, t) \psi(\vec{r}, \hat{\Omega}', E', t) \right] \\ + \nu \chi(E) \int_0^\infty dE' \Sigma_f(\vec{r}, E') \int_{4\pi} d\Omega' \left[\psi(\vec{r}, \hat{\Omega}', E', t) \right]. \end{aligned} \quad (2.13)$$

In order to make the Boltzmann transport equation independent of time, the neutron production by fissions can be modified by dividing it by a factor k . The transport equation is then:

$$\begin{aligned}
\left[\hat{\Omega} \cdot \vec{\nabla} + \Sigma_t(\vec{r}, E) \right] \psi(\vec{r}, \hat{\Omega}, E) &= \int_0^\infty dE' \int_{4\pi} d\Omega' \left[\Sigma_s(\vec{r}, \hat{\Omega}' \rightarrow \hat{\Omega}, E' \rightarrow E, t) \psi(\vec{r}, \hat{\Omega}', E') \right] \\
&+ \left(\frac{\nu}{k} \right) \chi(E) \int_0^\infty dE' \Sigma_f(\vec{r}, E') \int_{4\pi} d\Omega' \left[\psi(\vec{r}, \hat{\Omega}', E') \right]. \quad (2.14)
\end{aligned}$$

The maximum eigenvalue k is called k_{eff} and will be equal to one if the reactor is critical, and greater or less than one if it is supercritical or subcritical, respectively.

2.3 Deterministic and Probabilistic Methods

There are two methods that can be used for the simulation and modelling of neutron transport in a reactor. The first type is deterministic methods. These methods solve the Boltzmann transport equation numerically by applying approximations all throughout the modelled system. The second is probabilistic methods and uses Monte Carlo simulations to model the almost exact reactor system statistically. An example of deterministic methods used for the routine design and analyses of reactor cores, is the application of diffusion theory approximation, with spatial nodes that are course meshes, and two neutron energy groups. Such nuclear codes use pre-computed cross sections that have been generated for core-assembly regions. These methods provide accurate and computationally efficient capability for the analysis of low-heterogeneous. light water cooled reactors. We note that the Overall System for the Calculation of Reactors-4 (OSCAR-4) code used for analyses of SAFARI-1 is a deterministic capability that allows calculations using six neutron energy groups. Other deterministic methods solve the transport

theory equations, rather than the diffusion theory equations.

2.4 Q-Value Energy Components

The fission Q-value of a reactor is the sum of all the kinetic energy produced by radiation components in the reactor core. The energy released from fission comes from the fission products and radiation energy components namely, neutrons, prompt and delayed gamma rays, beta particles and neutrinos. There are two types of energy that can be recovered from the radiation components of fission; the first is the prompt energy released from neutrons and gamma rays, and the second is delayed betas and gammas as a result of fission product decay. The Q-value contains the energy of the neutrinos, but it is not recoverable.

Radiative capture also forms part of the recoverable Q-value though it is a separate nuclear reaction to fission. Radiative capture occurs when a neutron is absorbed by a nucleus in the core material. The absorption results in the formation of an excited compound nucleus that decays via gamma radiation. This radiation can deposit its energy then in the reactor, contributing to the recoverable energy produced from fission. Once the compound nucleus reaches its ground state, it may still be unstable and decay further via beta and/or gamma rays. Radiative capture is dependent on materials present in SAFARI-1. In particular, it depends on capture cross sections of the elemental nuclides as well as the neutron energy spectrum in the reactor core. This dependency makes this quantity reactor specific. Radiative capture can add significantly to the recoverable energy since it ranges from 3 - 12 MeV/fission (see Table 2.1).

In Table 2.1, the fission energy components that make up the Q-value are shown. A comparison of emitted energy and recoverable energy is given in reference [2].

The values shown in this table are only an approximation of the energy partition between the components and are specific to uranium-235. The actual energy partitions of the SAFARI-1 Q-value are given later in this work.

Table 2.1: Emitted and recoverable fission energy components of U-235 [MeV/fission] [2]

Component	Energy emitted	Energy recovered
Fission fragments	168	168
Fission product decay (FPD):		
(i) Beta-rays	8	8
(ii) Gamma-rays	7	7
Neutrinos	12	-
Prompt gamma-rays	7	7
Prompt neutrons	5	5
Radiative capture	-	3 - 12
Total	207	198 - 207

In Table 2.1, the second column shows the amount of heat energy released by the fission components per fission event. The third column shows the amount of energy that can be recovered from fission. The energy that can be recovered is converted into heat energy in the core and surroundings and is carried away by the reactor coolant. It can be seen that the total recoverable energy ranges between 198 - 207 MeV/fission. The main variable that determines the Q-value for a particular reactor is radiative capture. There are also other variables that might affect the Q-value such as the burn-up of fuel and the redistribution of core materials.

2.5 Spatial Heat Distribution in Reactor Components

The recoverable energy released in a fission event is deposited as heat in the reactor. This heat energy is distributed amongst the different radiation components in the reactor core. Depending on the type of particle released from fission, energy will be deposited in different locations of the reactor. This is due to the fact that radiation particles have different mean free paths. In Table 2.2, a description of the spatial heat distribution is given for U-235 and Pu-239, taken from ENDF/B-VII and reference [2]. A local heat distribution is within millimetres of the reaction that took place and a global heat deposition ranges between 10cm and a metre away from where the reaction took place. The radiative capture energies for U-235 and Pu-239 are not given in Table 2.2 because these quantities are dependent on materials in the reactor. Part of the aims of this work is to determine these quantities for SAFARI-1.

Table 2.2: Spatial heat distribution of U-235 and Pu-239 [MeV/fission]

Prompt energy	Range	Deposition	U-235	Pu-239
Q_{fp}	micrometres	local	166.97	175.55
Q_n	1cm - 10cm	global	5.34	6.07
$Q_{\gamma p}$	10cm - 1m	global	6.6	6.74
Energy released - FPD				
Q_{β}	millimetres	local	5.8	5.31
$Q_{\gamma d}$	10cm - 1m	global	5.6	5.17
Radiative capture				
$Q_{\gamma c}$	10cm - 1m	global	-	-
Capture beta	millimetres	local	-	-

2.6 Description of the SAFARI-1 Nuclear Reactor

SAFARI-1 is a 20 MW tank-in-pool Material Testing Reactor (MTR). The reactor uses light water as a coolant and reflector. SAFARI-1's main purpose is to produce radio-isotopes used for medical purposes. Molybdenum-99 (Mo-99) is the main isotope that is produced. The fuel used is 19.8% enriched uranium. The reactor core contains 26 fuel assemblies, 6 control rod assemblies, 7 molybdenum assemblies and several positions for the irradiation of isotopes. A beryllium reflector surrounds the reactor core. In the control rods, fuel is contained in the active region (lower zone) and cadmium in the absorbing region (upper zone). Water surrounds all the structural components in the core. The entire reactor core and reflector is contained in the core box which is contained in the reactor vessel. A schematic representation of the SAFARI-1 core is given in Figures 2.3 and 2.4.

A typical cycle in SAFARI-1 operating at full power is approximately 30 days long. During the cycle, molybdenum is constantly being irradiated and removed to maintain production output for clients. Since the molybdenum rigs contain fuel, the removal of such rigs consequently affects the power output of the reactor. The reactor remains critical (the number of neutrons produced = the number of neutrons absorbed) throughout the cycle. The purposes of some of the reactor components are given below:

- Aluminium core-box (Natural Al) - Acts as a shield against gamma radiation.
- Beryllium reflector - Reflects neutrons that escape back into the core.
- Moderator: light water (H_2O) - Slows down neutrons released from fission in order to cause more fission reactions.

- Absorbing region of the control rod - Contains cadmium which acts as a neutron poison to absorb neutrons and introduce negative reactivity in the core.
- Active region of the control rod - To increase reactivity worth of the control rod. Consider that, due to the follower, withdrawing a control rod not only removes neutron poisons from the core, but it also introduces a positive reactivity.
- Fuel in molybdenum assembly - Mo-99 is one of the bi-products of irradiating U-235, consequently, U-235 is also used as fuel.

2.7 SAFARI-1 Analysis Codes: OSCAR-4 and MCNP5

The two main codes used in support of the operation of SAFARI-1, are the Overall System for the Calculation of Reactors (OSCAR-4) code system and MCNP. The OSCAR-4 (OSCAR) code system, which is developed and maintained in the Radiation and Reactor Theory (RRT) Section of Necsca, is used for reactor reload design and core-follow analyses. It contains a three-dimensional, multi-group, nodal diffusion code which performs the calculations in a six-energy group structure for homogeneous nodes. During core depletion analysis, OSCAR tracks the depletion history of each fuel element in the reactor core [11]. For detailed transport calculations, the Monte Carlo code MCNP5 is used.

MCNP is a general-purpose Monte Carlo N-Particle transport code that is used in RRT for neutron, photon and coupled neutron/photon transport. MCNP's general geometry modelling capability and the use of point wise cross sections are amongst its main features that makes it applicable for the analysis of complex problems. In general, OSCAR and MCNP are used in conjunction, i.e. OSCAR

provides MCNP with the appropriate core depletion state for the detailed transport analysis. MCNP uses the ENDF data library for nuclide cross sections and nuclear reactions.

MCNP can be used to model the nuclear interactions between neutrons and several nuclei, as long as the cross sections are available in the nuclear data libraries. The nuclear interactions that are contained in the libraries are elastic and inelastic scattering, fission and radiative capture amongst several others. For this work, the radiative capture and fission cross sections were important. For gamma interactions with matter, MCNP can handle Compton scattering, pair production and the photo-electric effect. MCNP contains a tally feature that allows the user to calculate several reactor physics quantities. The heating tally feature was important for this work since they were used to calculate all the quantities that were needed to complete our objectives. The tally specifications are described in more detail in Chapter 3.

Like any other probabilistic code, MCNP requires the user to create an input file that defines several parameters. This can be done in any generic editor such as Notepad⁺⁺. The parameters that are defined in the input file are: the geometric model of the system (in this case the reactor configuration of SAFARI-1), the material description of each component in the system (this includes the library to be used for each nuclide), the source definition, and lastly, the tallies that are needed for the desired the result. Since MCNP uses probabilistic transport, it allows the user to specify the desired number of histories to run. In criticality calculations, during one cycle composed of several histories, the fission positions for the next cycle are stored in one file. During the inactive cycles, only the fission source is updated, and no contribution to the tallies is calculated. The number of inactive cycles is chosen by the user in order to obtain convergence of the fission source. The contribution to the tallies is done during the active cycles that start

after the inactive ones. The user can also specify the number of histories that are run within each cycle.

In the MCNP output file, the results of the tallies are given with appropriate units. Each tally result has an associated relative error. There are several checks printed in the output file that assists in determining whether the results have converged. An example is that of the table of 10 statistical checks performed for each tally, which can be seen in Appendix A-2. A summary of the checks on the tally results is as follows: mean behaviour, relative error (the value of the relative error and decrease rate is reported), and figure of merit or FOM which measures the efficiency of results and the PDF slope. For each check, there are three categories that describe the result, namely desired, observed and passed. All statistical checks should be passed for a set of results to be considered reliable. Simulations should, therefore, be run until all checks are passed.

The relative error of the result in MCNP is the fractional standard deviation of the results. To have confidence in the results, there are acceptable values for the fractional standard deviation given in literature [12]. For point detectors, the fractional standard deviation should be less than 5%, and for estimators, the fractional standard deviation should be less than 10%. If the fractional standard deviation is greater than 20%, it is an indication that the results are doubtful.

While MCNP proves advantageous for many particle transport applications, there are some limitations. Some calculations in MCNP are expensive in that they require a lot of calculation time. An example is shielding calculations that consist of large source volumes. MCNP is one of the best codes to use when performing complex shielding calculations; however, variance reduction techniques are required to improve the efficiency of the code when handling small region tallies independent of the source size.

2.8 MCNP Model of SAFARI-1

The MCNP model represents the actual three-dimensional physical geometries of the SAFARI-1 core. The model consists of volumetric cells that are made up of geometric surfaces. The cells make up the components of the reactor: for example, each fuel plate is defined by a separate cell. A collection of cells make up universes. It is easier to group similar components into the same universe. The surfaces and planes that comprise cells can assume complicated geometries and can be used to model complex reactor designs. Although SAFARI-1 does not have a complicated design, there are thousands of cells in the MCNP model.

The MCNP model of SAFARI-1 was also developed in the RRT Section of Necsa. An X-Y view of the MCNP model of SAFARI-1 can be seen in Fig. 2.3 which was viewed in the visual editor [13] package of MCNP. It includes the reactor core, core box, reactor tank and beam tubes. Inside the reactor tank, there is a grid plate with a rectangular arrangement of 8×9 positions where different assembly types can be loaded. The core is surrounded by a beryllium reflector and some aluminium and lead assemblies. In positions D6 and F6 (in Fig. 2.3), Isotope Production Rigs (IPRs) are present. For this work, they were filled with water [14], reason being, Necsa does not permit the IPR information to be available to the public. Six control rods are present in positions C5, C7, E5, E7, G5 and G7. Seven molybdenum positions are present in positions B6, B8, C3, D8, E3, F8 and G3. The rest of the positions in the core are fuel assemblies. The portion of lead and aluminium surrounding the reflector acts as shielding.

Fig. 2.4 shows the planar view of the model with the fuel, control rod elements and control rod fuel follower at the active regions of these components. The fuel that is used is Material Testing Reactor (MTR) type. Each fuel element contains 19 fuel plates. The fuel plates consist of a uranium-silicide-aluminium [U_3Si_2-Al]

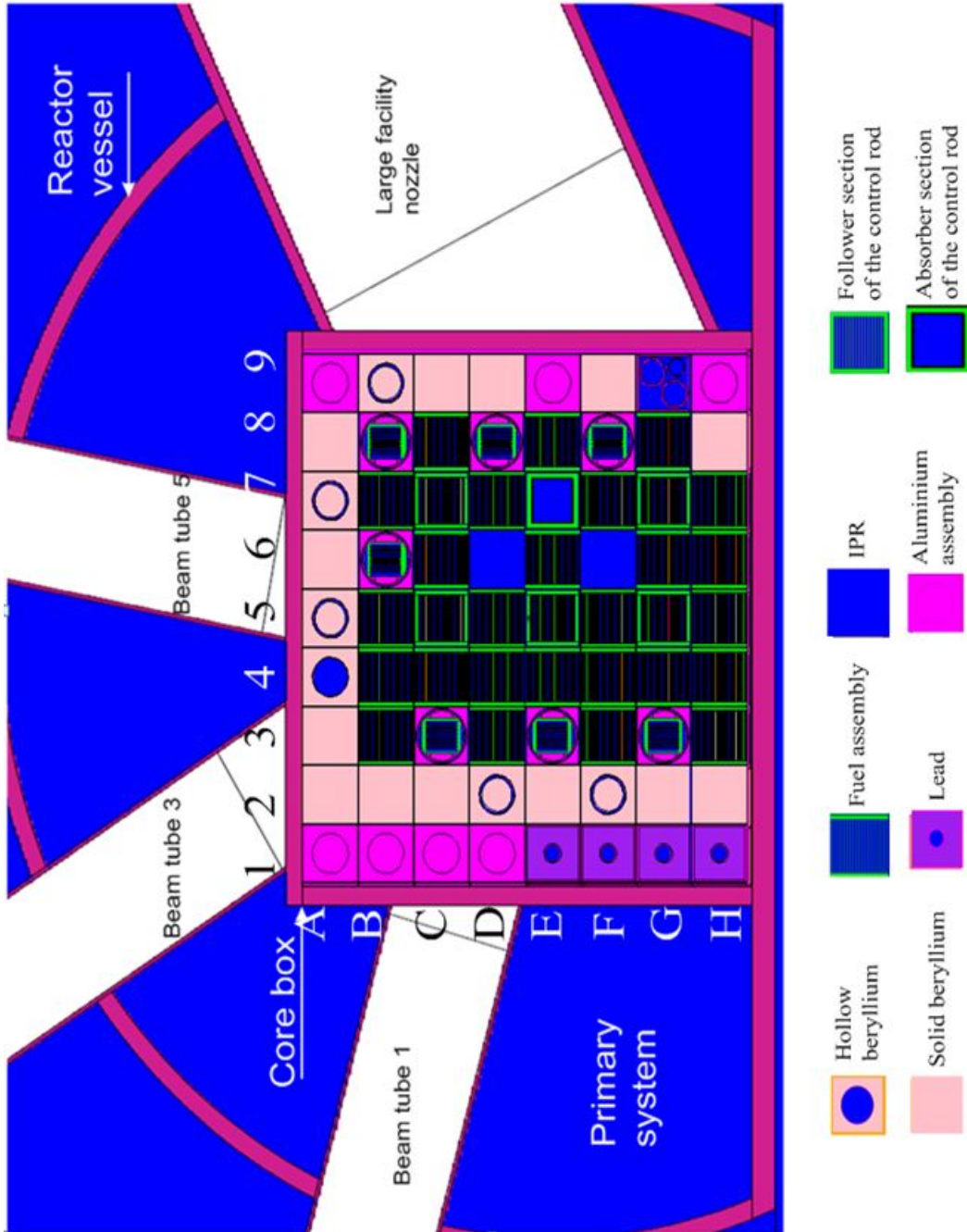


Figure 2.3: The MCNP SAFARI-1 core configuration

powder dispersed core, enclosed in an aluminium-alloy cladding.

Control rod assemblies consist of an upper absorber section and a lower fuel section connected through a rigid aluminium coupling mechanism. The absorbing section consists of an aluminium box that contains a cadmium layer as an absorber. The fuel section, which is also called the control rod follower, is similar to the fuel elements, but it is constructed inside an aluminium box and contains only 15 plates.

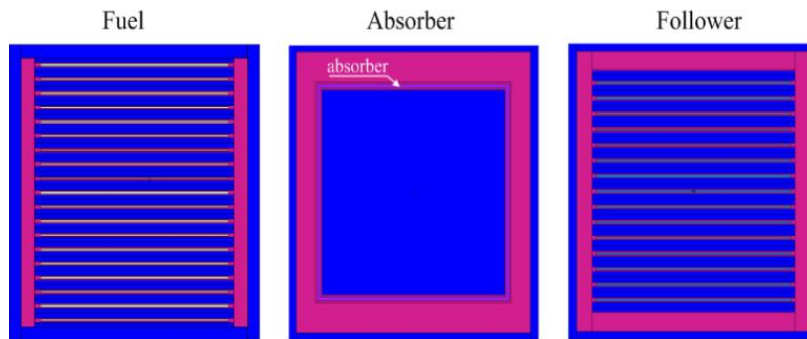


Figure 2.4: Planar view of fuel element with 19 plates, and the absorbing and follower region of the control rod respectively

2.8.1 Heating Tallies in MCNP

The F6 and F7 tallies built in MCNP are used to calculate heat energy deposition. MCNP does this by estimating the flux using a track-length estimator. The difference between the two tallies is that F6 calculates global heat deposition and F7 calculates local heat deposition. The F6 tally calculates the global heating by tracking all the particles that contribute to heating from birth to death. In order to calculate the heat deposition in the SAFARI-1 core, a coupled neutron-photon calculation was performed using the F6 tally. F7 calculates the heat produced from fission by assuming that all the energy created in a certain cell is deposited in that cell (i.e. locally). This includes heating from fission products, neutrons

and prompt gamma-rays.

2.8.1.1 The F6 Heating Tally

The equation that describes the F6 tally is given by [4]:

$$F6\left[\frac{\text{MeV}}{\text{g}}\right] = \frac{\rho_a}{m} \int_V \int_t \int_E \sigma_T(E) H(E) \phi(r, E, t) dE dt dV, \quad (2.15)$$

where,

ρ_a is the atomic density in atoms/barn-cm;

m is the cell mass in grams;

$\sigma_T(E)$ is the total neutron cross section in barns;

$H(E)$ is the heating number in MeV/collision; and

$\phi(r, E, t)$ is the scalar flux in $\text{cm}^{-2}\text{s}^{-1}\text{MeV}^{-1}$.

Below are the variations of the heating number for different cases of the F6 tally.

1. F6 tally for neutrons (F6:n)

$$H(E) = E - \sum_i P_i(E) [E_{\text{out}_i}(E) - Q_i + E_{\gamma_i}(E)], \quad (2.16)$$

where,

E is the incident neutron energy;

$P_i(E)$ is the probability of reaction i ;

$E_{\text{out}_i}(E)$ is the average neutron exiting energy for reaction i ;

Q_i is the Q-value of reaction i ; and

$E_{\gamma_i}(E)$ is the average gamma exiting energy for reaction i .

2. F6 tally for photons (F6:p)

$$H(E) = E - \sum_{i=1}^3 P_i(E)[E_{\text{out}}(E)], \quad (2.17)$$

where,

E is the energy of the incident neutron; and

$P_i(E)$ represents the probability of a reaction i , occurring some incident energy E .

The following types of reactions are represented by i : $i = 1$ is incoherent Compton scattering, $i = 2$ is pair production and $i = 3$ is photoelectric absorption.

2.8.1.2 The F7 Heating Tally

The equation that describes the F7 tally is given by [4]:

$$F7\left[\frac{\text{MeV}}{g}\right] = \frac{\rho_a}{m} \int_V \int_t \int_E \sigma_f(E) H(E) \phi(r, E, t) dE dt dV, \quad (2.18)$$

where σ_f is the fission cross section in barns. The heating number for F7 is the total prompt energy (fission products, prompt neutrons and gamma-rays) released per fission with respect to specific fissionable nuclides, e.g. the heating number for U-235 will be the prompt energy released per fission from U-235.

In the methodology chapter, the results that were obtained from the MCNP tallies are used systematically to calculate the components of the Q-value.

2.9 ENDF/B-VII and ENDF/B-VII.1 Data Libraries

The ENDF libraries contain important nuclear data, such as data for all neutron-induced reactions and incident neutron energies. This information is used by several nuclear industries for nuclear applications such as shielding, criticality and heating calculations. The data is stored in a computer-readable format which is used by several data processing programs in the main input file. All of the data in the ENDF libraries are calculated from benchmark experiments and theory. For this work, MCNP5 used the neutron cross-section data for fission and radiative capture from the ENDF/B-VII [15] data library. The ENDF/B-VII and ENDF/B-VII.1 are also used [16] to do an independent calculation of the Q-value.

CHAPTER 3

NUMERICAL EXPERIMENTS AND DATA EXTRACTION

“Prediction is very difficult, especially if it’s about the future.” —

Niels Bohr.

Chapter 3 will focus on the methodology used in calculating the fission Q-value and the spatial heat distribution in SAFARI-1. The first approach in calculating the Q-value uses MCNP5 exclusively. The second used the ENDF data libraries, ENDF/B-VII and ENDF/B-VII.1. Since radiative capture is not contained in the data libraries, in this approach the capture reaction rate in MCNP was used to calculate it. In the last section of the Q-value calculations, a comparison of Q-values between different stages in a typical 30-day cycle was done. This was achieved by enclosing the entire reactor system in one cell and doing a global heat calculation in MCNP5. This last step enables us to see if the Q-value changes with time during the cycle. Once the Q-value has been calculated, it is used to calculate the spatial heat distribution in SAFARI-1.

3.1 Fission Q-Value Calculation Using MCNP5

In the first part of the calculations, MCNP5 was used to perform a global heat deposition calculation. To do this, the F6 and F7 tallies were used. The methodology from [5] was followed. This specific calculation relied purely on MCNP because the heating values were obtained using MCNP5. The equations given in [5] were then used to calculate the Q-value components for SAFARI-1.

3.1.1 Procedure to Calculate the Q-value with MCNP5

The equations that were used to calculate the heat deposition from fission products, neutrons, and prompt and capture gammas are given below. For this specific calculation, the energy produced from delayed beta and gamma decay (fission product decay) were taken directly from the ENDF/B-VII library [16].

The Q-value calculations of the different tally results are given by:

$$Q_{F6:n} \text{ or } Q_{F6:p} \text{ or } Q_{F7} \left[\frac{\text{MeV}}{\text{fission}} \right] = v \left[\frac{\text{neutrons}}{\text{fission}} \right] \sum_{c=1}^{N_{\text{cell}}} (F6_c : n, F6_c : p, F7) \left[\frac{\text{MeV}}{g (\text{fission neutron})} \right] m_c [g], \quad (3.1)$$

where,

$F6_c : n, F6_c : p, F7$ are the results obtained from MCNP;

v is the average number of neutrons produced per fission also obtainable from the MCNP output;

m_c is the mass of a cell; and

N_{cell} is the total number of cells in the calculation.

MCNP outputs the tally results in units of [MeV/g/fission neutron]. From Eq. (3.1), it can be seen that the MCNP result is summed over the total number of cells present in the reactor multiplied by the mass of each cell. This result is multiplied by the number of neutrons released per fission ($\frac{\nu}{k_{eff}}$) to produce the Q-value in units of [MeV/fission]. The rest of the equations that were used to calculate the different Q-value components are given below:

$$Q_{F6:n} = Q_{fp} + Q_n, \quad (3.2)$$

$$Q_{F6:p} = Q_{\gamma p} + Q_{\gamma c}, \quad (3.3)$$

$$Q_{F7:n} = (Q_{fp} + Q_n + Q_{\gamma p}). \quad (3.4)$$

The prompt gamma Q-value can be calculated by subtracting the F6:n tally from the F7 tally. This can be seen in Eq. (3.5):

$$Q_{\gamma p} = Q_{F7} - Q_{F6:n}. \quad (3.5)$$

From Eq. (3.3), it can be seen that the Q-value for capture gamma rays can be found by subtracting the prompt gamma energy from the F6:p tally energy.

$$Q_{\gamma c} = Q_{F6:p} - Q_{\gamma p}. \quad (3.6)$$

Q_{β} and $Q_{\gamma d}$ are not present in the equations above and was taken from ENDF/B-VII [16]. These quantities are caused by the decay of fission products, and cannot be tallied by MCNP, and therefore, they were calculated from libraries.

For this work, the entire reactor configuration was enclosed in one cell. A heating calculation was run for the reactor core and the above equations were then used. The calculation was then run at day 3 and day 30 of a typical cycle in SAFARI-1. The reason for calculating the Q-value at the EOC was to study the effects of burn-up on the Q-value. The results are presented in Chapter 4.

3.2 Calculation of Energy Deposited from Radiative Capture ($Q_{\gamma c}$) Using MCNP5

Radiative capture depends on the materials present in the reactor core. As previously mentioned, this is the only contribution that cannot be approximated from nuclear data libraries. The process of radiative capture involves the capture of a neutron by the medium with a formation of an unstable compound nucleus. There is a subsequent release of nuclear binding energy through the emission of prompt gamma radiation when the compound nucleus de-excites. The deposition of the gamma energy in the core is the radiative capture Q-value. $Q_{\gamma c}$ may range from 3 - 12 MeV/fission [2]. After the capture of a neutron and release of prompt gamma radiation, the compound nucleus may still be in an excited state and decay further via delayed beta and gamma radiation. This energy must also be accounted for because it adds to the recoverable heat energy in the reactor core.

To calculate the recoverable energy from radiative capture, the radiative capture reaction rate of each material that contributes substantially to the heating was calculated in MCNP5 and the result was multiplied by the number density of the material [17]. We then used the binding energy of the material to obtain the heat energy produced from radiative capture.

3.2.1 Description of the Radiative Capture Reaction Rate in MCNP

The Radiative Capture Reaction Rate (RCRR) is given by Eq. (3.7):

$$RCRR_i = N_i \int \varphi(r, E) \sigma_{ci}(r, E) dEdV, \quad (3.7)$$

where:

N_i is the number density of isotope i [atoms/cm³];

ψ is the energy dependent neutron flux [neutron/cm²]; and

σ_{ci} is the radiative capture cross section for isotope i [barn].

We used the Segment Divider (SD) card=1. The SD card is used to supply the tally with specific information that relates to tally such as the volume, area or mass of the cell. SD equals one implies that the capture reaction rate is divided by one instead of by the cell volume. The MCNP results for the capture reaction rate are given in units of [neutrons.barn.cm]. Multiplying this result by the number density [atoms/barn.cm], we get a unit of [reactions]. MCNP produces results per neutron born per second in the system, and therefore, the reaction rate will have units of [reactions/neutron born in the system].

The isotopes forming the i th element in Eq. (3.7) are from the elements that contribute substantially to the heating produced from radiative capture in the core. Table 3.1 lists the elements contained in the components of the SAFARI-1 core.

From Ta

From Table 3.1, it can be seen that the majority of the core consists of aluminium and hydrogen. There are also other materials present in the core; however for this

Table 3.1: List of elements present in the SAFARI-1 reactor core

Element	Component
Hydrogen	Coolant, Primary system
Aluminium	Fuel plates, Structural assemblies
Cadmium	Control rod, Irradiation devices
Silicon	Fuel meat, Follower of control rod
Uranium	Fuel meat, Follower of control rod
Beryllium	Reflector

work, only the materials that contribute majorly to the heating in the reactor are considered as opposed to all of the materials.

3.2.2 Calculation of $Q_{\gamma c}$ using the Radiative Capture Reaction Rate

We first normalise the RCRR by multiplying it by $[\nu/K_{\text{eff}}]$ (neutrons produced per fission), and obtain the total number of capture reactions produced per fission in the reactor. Binding energy is released during each radiative capture. We can calculate the binding energy of a capture reaction by subtracting the mass of the target nucleus plus the mass of the neutron (8.07 MeV) from the product nucleus mass. If we multiply the number of capture reactions produced per fission for each nuclide by its binding energy per capture, we obtain the energy released by capture per fission in units of MeV/fission.

The reasoning for the above is as follows: when a neutron is captured by a nucleus in a core material, a compound nucleus is formed. The excitation energy of the compound nucleus is due to the binding energy and the kinetic energy from the incident neutron. The prompt gammas released in the de-excitation of the compound nucleus end up as heat energy in the reactor core. The kinetic energy of the incoming neutron is accounted for in the calculation of prompt and delayed

neutron energy from fission, and therefore we do not consider it in this section.

In some cases, after decaying to its ground state, the compound nucleus is still excited and will decay further via delayed beta and/or gamma emission. This delayed energy contribution when produced by short-life nuclides adds additional heat energy to the core.

Table 3.2 lists the various nuclides with their associated binding energies that were used in calculating $Q_{\gamma c}$. The binding energies were calculated using the masses of the nuclides presented in Table 3.2 which were taken from reference [3].

Table 3.2: Binding energies of the nuclides present in SAFARI-1 [3]

Target element	Target isotope	Compound nucleus	Binding energy (MeV)
Aluminium	Al-27	Al-28	7.7307
Silicon	Si-28	Si-29	8.4751
	Si-29	Si-30	10.617
	Si-30	Si-31	6.5940
	Hydrogen	H-1	H-2
Cadmium	Cd-106	Cd-107	7.9243
	Cd-108	Cd-109	7.3197
	Cd-110	Cd-11	6.9741
	Cd-111	Cd-112	9.3979
	Cd-112	Cd-113	6.5401
	Cd-113	Cd-114	9.0421
	Cd-114	Cd-115	6.1386
	Cd-116	Cd-117	5.7669
Uranium	U-235	U-236	6.1386
	U-238	U-239	5.7669
Beryllium	Be-9	Be-10	6.8149

The total number of capture reactions per fission for each nuclide in Table 3.2 was multiplied by the binding energy of the compound nucleus per reaction, and the energy released per radiative capture for each nuclide was obtained.

For the decay energy of unstable compound nuclei, based on the nuclides in Table 3.2, we only consider the beta decay from Al-28, Cd-113, Cd-115 and Cd-117. The reason is that these are short-lived nuclides and can contribute to the deposited

energy in the form of beta and gamma decay. To account for this energy, the decay energy of each nuclide presented in Table 3.3 was added to the binding energy of the respective nuclide. Table 3.3 lists the decay and binding energies of the unstable nuclei that were considered for this work.

Table 3.3: Decay energies of unstable nuclei in SAFARI-1

Unstable nucleus	Decay energy (MeV/reaction)	Binding energy (MeV)
Al-28	4.640	7.7307
Cd-113	0.323	6.5401
Cd-115	1.452	6.1386
Cd-117	2.525	5.7669

The decay energies in Table 3.3 were taken from Janis 4.0 [1]. In the case of Al-28, the Q-value of Al-28 to Si-28 is 4.64 MeV (from the mass excess); however, we cannot use this value as it stands. Of that 4.64 MeV, the beta-decay component is 1.2418 MeV and the gamma-decay component is 1.77 MeV. The rest of the energy is lost to neutrinos. The total decay energy from beta and gamma contributions for Al-28 that adds to the Q-value of the reactor is therefore only 3 MeV. All of the decay energy for the cadmium nuclides are due to beta-decay. The results obtained for these calculations are given in Chapter 4.

3.3 Calculation of Fission Q-Value Components Using ENDF/B-VII and ENDF/B-VII.1

In Section 3.1, the way in which MCNP can be used to calculate the fission Q-value was discussed. The only energy released per fission that depends on a specific reactor is the energy due to radiative capture. In this section, we discuss the rest of the energy components that can be obtained from the data libraries. Two approximations are used, namely the ENDF/B-VII and the ENDF/B-VII.1

data libraries. The ENDF-VII library makes use of formulae derived from definitions [16] and ENDF-VII.1 makes use of a polynomial approximation proposed by Madland and Nix [15]. Both approximations use the incident neutron energy that produces fission (E_n), to calculate the Q-value.

3.3.1 Calculation of Q-value Components using ENDF/B-VII Equations

The equations used from ENDF to calculate the Q-value energy components are as follows:

$$E_{FR}(E_n) = E_{FR}(0), \quad (3.8)$$

where

E_{FR} is the kinetic energy of the fission fragments:

$$E_{NP}(E_n) = E_{NP}(0) + 1.307E_n - 8.071 * 10^6[\nu(E_n) - \nu(0)], \quad (3.9)$$

where

E_{NP} is the kinetic energy of the prompt fission neutrons, and

ν is the total number of neutrons released per fission reaction in the reactor core:

$$E_{ND}(E_n) = E_{ND}(0), \quad (3.10)$$

where

E_{ND} is the kinetic energy of the delayed fission neutrons:

$$E_{\text{GP}}(E_n) = E_{\text{GP}}(0), \quad (3.11)$$

where

E_{GP} is the energy released from prompt gamma rays:

$$E_{\text{GD}}(E_n) = E_{\text{GD}}(0) - 0.075E_n, \quad (3.12)$$

where

E_{GD} is the energy released from delayed gamma rays:

$$E_{\text{B}}(E_n) = E_{\text{B}}(0) - 0.075E_n, \quad (3.13)$$

where

E_{B} is the energy released by delayed beta-rays; and

$$E_{\text{NU}}(E_n) = E_{\text{NU}}(0) - 0.1E_n, \quad (3.14)$$

where

E_{NU} is the energy lost to the neutrinos.

For the calculation of the mean energy of the neutrons producing fission, E_n , the total Fission Reaction Rate (FRR) was calculated with MCNP5 in the 172 energy groups of the X-MAS structure as shown in reference [18]. E_n is given by Eq. (3.15).

$$E_n = \frac{\int_0^\infty E\phi(E)\sigma_f(E)dE}{\int_0^\infty \phi(E)\sigma_f(E)dE} = \frac{\sum_{g=1}^{172} \int_g E\phi(E)\sigma_f(E)dE}{\sum_{g=1}^{172} \int_g \phi(E)\sigma_f(E)dE} \quad (3.15)$$

$$\approx \frac{\sum_{g=1}^{172} \bar{E}_g \phi_g \sigma_{fg}}{\sum_{g=1}^{172} \phi_g \sigma_{fg}} = \frac{\sum_{g=1}^{172} \bar{E}_g \text{FR}R_g}{\sum_{g=1}^{172} \text{FR}R_g},$$

where,

g is the energy group number,

$\phi(E)$ is neutron flux in [neutrons.cm⁻².s⁻¹],

$\sigma_f(E)$ is the microscopic fission cross section which has units [cm²], and

$\phi_g = \int_{\Delta E_g} \phi(E) dE$ is the total neutron flux in group g [neutrons.cm⁻².s⁻¹],

σ_{fg} is the fission cross section in group g , cm²

\bar{E}_g is the mid energy of group g , [MeV]

3.3.2 Calculation of Q-value Components using ENDF/B-VII.1

A new representation of calculating the Q-value energy components was found recently by Madland, and is given in [16]. It was found that, for the prompt energy released in fission, the average of the total prompt energy is given by Eq. (3.16):

$$E_d(E_n) = E_{\text{FR}}(E_n) + E_{\text{NP}}(E_n) + E_{\text{GP}}(E_n), \quad (3.16)$$

where E_d is the energy deposition from fission, namely, fission products, prompt neutrons and prompt gamma rays.

Equation (3.16) is based on actual experimental measurements from the Los Alamos model (Madland and Nix) [19]. The observations were as follows: "to first order, the components in Eq. (3.16) can be represented by linear or quadratic polynomials as a function of E_n ." Equation (3.16) may therefore be represented as:

$$E_{\text{COMP}}(E_n) = c_0 + c_1 E_n + c_2 E_n^2, \quad (3.17)$$

where E_{COMP} is the energy of the Q-value component. The recommended 0th order coefficients for U-235, U-238 and Pu-239 are given in Table 3.4, which was taken directly from Janis 4.0 [1].

Table 3.4: Madland's recommended energy release polynomial coefficients [MeV]

Nuclide	Parameter	c_0	c_1	c_2
U-235	E_{FR}	169.13	-0.2660	0.0
	E_{NP}	4.838	0.3004	0.0
	E_{GP}	6.600	0.0777	0.0
	E_{ND}	0.0074	0	0
	E_{GD}	6.33	-0.075	0
	E_{B}	6.5	-0.075	0
	E_{NU}	8.75	-0.1	0
U-238	E_{FR}	169.8	0.3230	0.004206
	E_{NP}	4.558	0.3070	0.0
	E_{GP}	6.680	0.1239	0.0
	E_{ND}	0.018	0	0
	E_{GD}	8.25	-0.075	0
	E_{B}	8.48	-0.075	0
	E_{NU}	11.39	-0.1	0
Pu-239	E_{FR}	175.55	0.4566	0.0
	E_{NP}	6.128	0.3428	0.0
	E_{GP}	6.741	0.1165	-0.0017
	E_{ND}	0.299	0	0
	E_{GD}	5.17	-0.075	0
	E_{B}	5.31	-0.075	0
	E_{NU}	7.14	-0.1	0

Madland's recommendation for the coefficients of U-235, U-239 and Pu-239 have been implemented in the most recent revision of the ENDF library-ENDF/B-

VII.1. Using the methodology explained in Section 3.2.1, the incident energy was found and Eq. (3.17) was used to calculate the Q-value components. These results are presented in Chapter 4.

3.4 Spatial Heat Distribution in SAFARI-1

Apart from the Q-value of a reactor, another important quantity is needed, that is, the spatial heat distribution in fuel and non-fuel regions. The spatial heat distribution is the amount of heat energy deposited in different regions of the reactor. It is important to know this distribution so that cooling can be implemented in regions where the heat deposition is higher. We can calculate the spatial heat distribution by using heating tallies in MCNP5. The kinetic energy of the fission fragments is deposited in the fuel. Neutrons and gammas deposit their energy throughout the reactor system. From fission product decay, beta particles deposit their energy in the fuel. From radiative capture, gammas deposit their energy throughout the reactor system and delayed betas deposit their energy where the capture occurs, i.e. in the fuel or surrounding region. In this section, a method of calculating the spatial heat distribution using MCNP5 is explained. The methodology in reference [5] was used.

3.4.1 Calculation of the Spatial Heat Distribution Due to Prompt Energy Components

Since MCNP outputs heating results per neutron born in the system, we can apply a normalisation by using the equation for the heating rate. This is given by Eq. (3.18):

$$\text{Heat}_i \left[\frac{\text{W}}{\text{g}} \right] = \frac{F6 : n \text{ or } F6 : p \text{ or } F7 : n \left[\frac{\text{MeV}}{\text{fission neutron}} \right] P[\text{W}] \nu \left[\frac{\text{n}}{\text{fission}} \right]}{Q \left[\frac{\text{MeV}}{\text{fission}} \right] k_{\text{eff}}}. \quad (3.18)$$

The results of Eq. (3.18) are in units of [W/g]. If we use the SD=1 card (see Appendix A-1), the MCNP results will be in MeV/fission, instead of MeV/g, then we can obtain the results in Watts. If requested in the input file, MCNP will output the mass of a cell. The mass can also be calculated analytically since we know the dimensions of the cell and material contained in the cell. The density can be used to find the mass. For the power term, the power of SAFARI-1, being 20 MW, was used. The Q-value is the reactor-specific Q-value of SAFARI-1, and the number of neutrons released per fission, which was 2.457, could be obtained from the MCNP output file.

The F6:n and the F7 tallies were used to calculate the heat produced from fission products and neutrons. The F6:p tally was used to calculate the heat due to prompt and capture gamma-rays. These tallies can be used to calculate the heat deposition in different components of the reactor.

3.4.2 Calculation of the Spatial Heat Distribution due to Fission Product Decay

A problem arises when calculating the heating from fission product decay i.e. delayed gamma and beta decay. MCNP5 cannot calculate delayed gamma or beta decay from fission product decay; however, different methods can be used to calculate these contributions. We can calculate the heating due to fission product decay by manipulating the tally that calculates prompt and capture gamma-rays which is the F6:p tally. In order to follow this approach with MCNP5, an as-

sumption was made that the prompt gamma spectrum is the same as the delayed gamma spectrum from reference [5]. The heating from delayed gammas $H_{\gamma d}$ was then calculated at some point as a function of the energy produced from prompt gammas at the same point. This relation is given in Eq. (3.19):

$$Heat_{\gamma d}[W] = \frac{Q_{\gamma d}}{Q_{\gamma p}} Heat_{\gamma p}, \quad (3.19)$$

where, $Q_{\gamma p}$ and $Q_{\gamma d}$ are the Q-values for prompt and delayed gammas respectively. The energy $H_{\gamma p}$ can be obtained with MCNP5 using the Photon-production bias card (PIKMT) card in order to select the nuclides that produce gammas. This can be seen in Appendix A-1. Equation (3.19) is already in the desired units, i.e. Watts, and therefore, no normalisation is required.

The F7 tally was used to calculate the heating due to beta particles from fission product decay. We assume that beta particles produced from fission product decay is deposited only in the fuel (local deposition). We can calculate the heating due to beta decay using Eq. (3.20). The units will be the same as that of the F7 tally. We can then apply the normalisation equation Eq. (3.18) to obtain the heat contribution in Watts.

$$Heat_{\beta} = \frac{Q_{\beta}}{Q_{fp} + Q_n + Q_{\gamma p}} F : 7 \quad (3.20)$$

where,

Q_{β} , Q_{fp} , Q_n and $Q_{\gamma p}$ are the fission Q-value components presented in Chapter 3. The last component that is considered, is energy produced from the activation of Al-28 and Cd nuclides as shown in Table 3.3. To calculate the heat contribution, we can use the Q-value obtained for this decay in MeV/fission and use the normalisation equation, Eq. (3.18) to convert the quantity to Watts.

Once the heating components have been calculated, a percentage calculation of the distribution of the heat in the reactor components can be done.

CHAPTER 4

RESULTS AND DISCUSSION

“I am frequently astonished that it so often results in correct predictions of experimental results.” — Murray Gell-Mann

The current chapter presents the fission Q-value obtained for SAFARI-1 by applying the procedures described in Chapter 3.

We first take a look at calculating the Q-value using a global heat calculation with MCNP5. This is done by enclosing the entire system in one cell and using a combination of the F6 and F7 tallies. Since MCNP5 cannot calculate the quantities Q_β and $Q_{\gamma d}$, these quantities were calculated using the ENDF/B-VII data libraries [16].

Another approach used to calculate the fission Q-value of SAFARI-1 used ENDF/B-VII and ENDF/B-VII.1 data libraries for all energy contributions except for the energy produced by radiative capture $Q_{\gamma c}$. It was therefore calculated using the RCRR obtained with MCNP5 and the binding energies of the involved nuclides as explained in Section 3.2.

A comparison of the fission Q-values obtained for different days within a typical

SAFARI-1 cycle is presented to analyse how burn-up affects the Q-value. Finally the spatial heat distribution in SAFARI-1 was calculated.

All calculations were done with MCNP5 using the approved MCNP model for SAFARI-1 [14]. For all Q-value and spatial heat calculations that were done, the input files used were taken from an actual past cycle in the reactor. The data came from cycle C1502-1, which was the second operational cycle of SAFARI-1 in the year 2015. The calculations performed at BOC were done at three days within the cycle in order to have equilibrium of xenon. Xenon is a bi-product of iodine in the reactor. In order to maintain equilibrium in the reactor core, the rate of production of iodine must be equal to the rate of removal of iodine. Xenon equilibrium is dependent on iodine equilibrium. Once the reactor is shut down, the production of iodine is seized. At three days into the cycle, there is equilibrium of xenon.

The EOC calculations were done for day 30 of operation within the cycle. This was a typical cycle because there were no SCRAMS (forced shut-downs) during this cycle. All MCNP5 calculations were done in eigenvalue mode, with 1 000 active cycles, using 200 000 histories per cycle. One hundred inactive cycles were chosen so that MCNP starts the active cycles with a well-converged fission source. In this work, statistical error propagation was not taken into account because the statistical errors that were associated with the MCNP results were all less than 0.1% of the result.

In Section 4.1, the results obtained for the global one-cell calculation in MCNP5 are shown together with the approximations from the data libraries for the components that MCNP5 cannot calculate (Q_β and $Q_{\gamma d}$). Section 4.2 presents the results obtained for the calculation of $Q_{\gamma c}$ through the capture reaction rates obtained with MCNP5 as well as the heating contribution from beta decay of the

short-life activated materials. The Q-value results that were obtained using the ENDF/B data libraries are shown in Section 4.3. Finally, Section 4.4 gives a comparison of Q-values obtained for different days within a typical cycle of SAFARI-1. The last section concludes the results chapter by showing the results obtained for the spatial heat distribution in SAFARI-1 and the percentage heat distribution in the fuel and the rest of the reactor components.

4.1 Q-Value Results Using MCNP5

Table 4.1 presents the results obtained for SAFARI-1 using the procedure described in Section 3.1. This was done by enclosing the entire core in one cell and performing a global heat calculation using the F6 and F7 tallies in MCNP5. Since MCNP5 cannot calculate the heat contribution from delayed gammas coming from fission product decay and beta radiation from fission, the ENDF/B-VII library was used as explained in Section 3.3.1. In the second column of the table below are the Q-value results for U-235 [20].

It is likely that some cells may be missed when calculating the Q-value by manually inputting cells in a tally. Consequently, the entire reactor configuration was enclosed in one cell. This ensured that no cells were missed when doing the MCNP calculation, and adds to the credibility of the results. Some tallies in cells inside the system were calculated in order to have a measure of control on the convergence of the calculations.

Table 4.1: Q-value results obtained using MCNP5 and ENDF/B-VII [MeV/fission]

Q-value components	Q-value	ENDF/B-VII for U-235
$Q_{FP} + Q_n$	174.500	174.053
Q_β (fission product decay)	6.472	6.500
$Q_{\gamma d}$	6.303	6.330
$Q_{\gamma p}$	6.750	6.600
Total	194.025	193.483
$Q_{\gamma c}$	6.610	-
Delayed beta and gamma (capture)	0.560	-
Fission Q-value	201.200	

The one-cell calculation using the energy deposition tallies in MCNP5 were used to calculate the heat contributions from fission products and neutrons, prompt and delayed gamma-rays, and gamma-rays from radiative capture. The heat contribution from betas and delayed gammas was calculated using Eq. (3.12) and Eq. (3.13). If we compare the MCNP results with the ENDF results, we see that fission products and neutrons, beta-rays, and delayed gammas compare well with the ENDF data base. However, the MCNP result for prompt gammas differs from ENDF by 2%. This is a small difference, and so it will not affect the Q-value significantly. The heating from delayed beta and gamma decay from capture is as a result of the decay of irradiated materials with a short life. This quantity cannot be calculated with MCNP5 and was obtained manually. The reasoning on how this value was obtained will be explained in Section 4.2. The value that was obtained for delayed betas and gammas is 0.560 MeV/fission (see Table 4.2). Considering that most of the fissions are produced in U-235 in SAFARI-1, the MCNP results are satisfactory since they compare well with the Q-value of U-235 from the ENDF/B-VII library.

4.2 Calculation of $Q_{\gamma c}$ by the Activation of the Reactor Components

As explained in Section 3.2, it was proposed that the method of calculating the energy released from radiative capture could be calculated as in reference [6]. We calculated this by multiplying the capture reaction rate and the binding energy of each material that contributes majorly to the heating in the reactor. Table 4.2 presents the results obtained from the $Q_{\gamma c}$ calculation.

Table 4.2: The Q-value result obtained for radiative capture ($Q_{\gamma c}$) and activation heating from beta decay [MeV/fission]

Element	Radiative capture	Delayed betas and gammas	Total
Aluminium	1.40	0.54	1.94
Hydrogen	1.76	0.00	1.76
Uranium-235	1.20	0.00	1.20
Uranium-238	0.56	0.00	0.56
Silicon	0.0127	0.00	0.0127
Beryllium	0.14	0.00	0.14
Cadmium	0.60	0.022	0.63
Total	6.06	0.56	6.24

In Table 4.2, we see that the energy produced by gamma rays due to radiative capture is 6.06 MeV/fission. This energy is produced immediately after a capture. Some activated nuclides continue to be in an excited state after the emission of the gamma-ray, and decay by emitting beta rays. This energy, for short-lived activated nuclides was calculated, and 0.56 MeV/fission was obtained. This quantity was calculated by adding the energy from delayed betas and gammas of the nuclides shown in Table 3.3 to the binding energy of the respective nuclides. Using MCNP5, the heating due to radiative capture produced by gamma rays were calculated as 6.61 MeV/fission, see Table 4.1. The difference between the two values obtained for $Q_{\gamma c}$ is 0.55 MeV/fission. We can account for the difference by under-

standing that only materials that contributed majorly to the heating and not all the materials present in the reactor core were considered. For delayed beta-decay, only the short-lived isotopes of uranium and cadmium were considered.

4.3 Q-Value Results Obtained Using ENDF/B-VII and ENDF/B-VII.1

In Section 3.3, we discussed a method of obtaining the average energy of the incident neutron producing fission in SAFARI-1. E_n was calculated, and a value of 2.915E-02 MeV was obtained. In the next step, the Q-value components for U-235, U-238 and Pu-239 was calculated as a function of E_n by using the equations given in Sections 3.3.1 and 3.3.2. These components are shown in the Table 4.3 for ENDF/B-VII and ENDF/B-VII.1. The Q-value components for U-235, U-238 and Pu-239 were calculated since these isotopes are the only ones with a significant fission reaction rate in SAFARI-1.

In order to calculate the fission Q-value, the percentage that each isotope contributes to the total FRR in SAFARI-1, using MCNP5 was calculated. Table 4.4 gives the percentage contributions to fission for the fission reaction rates at BOC (day 3).

Table 4.4: Fission reaction rate of fuel nuclides in SAFARI-1

Isotope of uranium	% FRR
U-235	96
U-238	1
Pu-239	3
Total	100

Using the results shown in Tables 4.3 and 4.4, the weighted averages of each Q-value component of U-235, U-238 and Pu-239 were calculated and added together

Table 4.3: Q-value components of fission obtained using the ENDF/B data libraries for various nuclides [MeV/fission]

ENDF Fission components	U-235		U-238		Pu-239	
	ENDF/B-VII	ENDF/B-VII.1	ENDF/B-VII	ENDF/B-VII.1	ENDF/B-VII	ENDF/B-VII.1
E_{FR}	169.130	169.130	169.570	169.800	175.550	175.550
E_{NP}	4.910	4.838	4.804	4.558	6.093	6.128
E_{ND}	0.007	0.007	0.018	0.018	0.003	0.003
E_{GP}	6.600	6.600	6.680	6.680	6.741	6.471
E_{GD}	6.330	6.330	8.250	8.250	5.170	5.170
E_B	6.500	6.500	8.480	8.480	5.310	5.310

to give the final Q-values. These results are shown in Table 4.5.

Table 4.5: Weighted averages of U-235/U-238/Pu-239 [MeV/fission]

ENDF fission components	ENDF/B-VII	ENDF/B-VII.1
E_{FR}	169.347	169.265
E_{NP}	4.949	4.872
E_{ND}	0.007	0.007
E_{GP}	6.605	6.602
E_{GD}	6.303	6.304
E_{B}	6.472	6.474
Total excluding neutrinos	193.683	193.524

To include radiative capture, the values of $Q_{\gamma\text{c}}$ and delayed beta-decay were used from the radiative capture reaction rate using MCNP5 as shown in Section 4.2. Table 4.6 shows the fission Q-values obtained using the ENDF/B libraries and the radiative capture reaction rate.

Table 4.6: Q-value results obtained for ENDF/B [MeV/fission]

Q-value components	ENDF/B-VII	ENDF/B-VII.1
$Q_{\text{fp}} + Q_{\text{n}}$	174.303	174.140
Q_{β}	6.472	6.474
$Q_{\gamma\text{d}}$	6.303	6.304
$Q_{\gamma\text{p}}$	6.605	6.602
$Q_{\gamma\text{c}}$	6.060	6.060
Beta-decay (delayed)	0.560	0.560
Total	200.303	200.140

In Table 4.6, we see that the Q-value obtained using the ENDF/B-VII.1 approximation is 200.140 MeV/fission and the Q-value obtained for the ENDF/B-VII approximation is 200.303 MeV/fission. These two values are close to each other. If we compare each Q-value component, we see that none of the differences add any major discrepancies between both sets of results. The ENDF/B-VII approximation gives us slightly higher values than the ENDF/B-VII.1 approximation. The biggest difference is between fission products and neutrons. The ENDF/B-

VII is higher by 0.16 MeV/fission. All the other differences are in the order of 10^{-3} .

With MCNP5, we obtained a Q-value of 201.20 MeV/fission. Using the ENDF/B-VII equations, we obtained 200.30 MeV/fission. Therefore, we calculated the final Q-value as an average of the MCNP and ENDF/B-VII Q-values with an associated standard error. The final Q-value result for SAFARI-1 is 200.8 MeV/fission ± 0.6 MeV/fission.

4.4 Comparison of Q-Values at Different Stages in a Cycle

During an operational cycle, there will be burn-up of fuel that results in different compositions of nuclides and isotopes. This phenomenon could affect the Q-value. In order to study this effect, MCNP5 was used to calculate the Q-value at BOC (day 3) and EOC (day 30) of a typical cycle in SAFARI-1. The same cycle was used as in the calculation in Section 4.1. The results for the Q-value during different stages of a cycle are given in Table 4.7.

Table 4.7: Comparison of Q-values for different stages in a typical SAFARI-1 cycle [MeV/fission]

Q-value component	BOC (Day 3)	EOC (Day 30)
$Q_{fp} + Q_n$	174.5	174.3
Q_β	6.5	6.5
$Q_{\gamma d}$	6.3	6.3
$Q_{\gamma p}$	6.8	6.7
$Q_{\gamma c}$	6.6	6.4
Beta-decay (delayed)	0.56	0.56
Total	201.3	200.8

From Table 4.7, it can be seen that the Q-value remains fairly constant at any point in the cycle. The difference between the two Q-values is 0.5 MeV/fission

which is around 0.25% of the fission Q-value. SAFARI-1 uses 19.8% enriched fuel, and the majority of fissions are due to U-235, therefore the change in composition of the fuel nuclides does not affect the total reaction rate significantly enough to conclude that the fission Q-value cannot be calculated at any point in the cycle. Note that the ENDF/B-VII data library was used for the $Q_{\gamma d}$ and Q_{β} quantities. The beta decay from activation was taken from the radiative capture calculation shown in Section 4.2.

4.5 Results Obtained for the Spatial Heat Distribution in SAFARI-1

The spatial heat distribution is an important calculation for safety analyses because it allows for the quantification of the heat distribution in different components of the reactor. This is important to ensure that overheating does not occur and cooling can be applied in the appropriate region of the core. The procedure that was followed to calculate the spatial heating was described in Chapter 3.4. A Q-value of 200.8 MeV/fission was used to normalise the MCNP results to the power of SAFARI-1. For this calculation, the heating tallies in MCNP was used. The Q-value components that were required to calculate the heat produced from beta and prompt gamma rays were taken from ENDF/B-VII. The results obtained are presented in Table 4.8.

Table 4.8: Energy deposition in different components of SAFARI-1 [MW]

Components	Fuel meat	Core excluding fuel meat	Reflector	Core box	Water surrounding core box	Total
$P_{fp} + P_n$	17.046	0.273	0.045	0.002	0.025	17.391
P_β	0.643	0.00	0.00	0.000	0.000	0.643
$P_{\gamma d}$	0.223	0.277	0.081	0.002	0.023	0.606
$P_{\gamma p} + P_m$	0.345	0.497	0.162	0.067	0.135	1.205
Total	18.257	1.047	0.288	0.071	0.183	19.845

The fuel meat includes the fuel from fuel elements, the followers in the control rods and the fuel region in the molybdenum assemblies. The core excluding fuel includes the rest of the components in the core. The reflector and core box includes the entire region surrounding the reactor core.

The heat contribution from radiative capture beta decay is not shown in Table 4.8, because it comes from all the components of aluminium. Since aluminium makes up most of the structural components, we cannot say exactly from where this heating comes. Consequently, it was added to the total power. To calculate this, the normalisation equation (Eq. (3.18)) given in Section 3.5 was used. The result obtained for delayed betas from capture in Section 4.2 (0.56 MeV/fission) was used to calculate the heat contribution in MW. A result of 0.137 MW was obtained for the heat contribution of delayed beta-rays due to radiative capture.

For SAFARI-1, the total heating using MCNP5 was calculated as 19.845 MW. The heat due to beta decay from activation was calculated to be 0.137 MW. Therefore, the sum of the results is the total heat deposited in SAFARI-1 which is 19.982 MW.

The percentage heat distribution between fuel and non-fuel is as follows:

- 97% deposited in the fuel (entire core: fuel meat, core excluding fuel meat), and
- 3% deposited in the surrounding region (reflector, core box and water surrounding the core).

Since SAFARI-1 is a 20 MW reactor, this result is consistent with the operating power of the reactor.

CHAPTER 5

CONCLUSIONS

“It always seems impossible until it’s done.” — Nelson Mandela

Two methods of calculating the reactor-specific Q-value were presented in this work. The first method used MCNP5 and the second method used the ENDF/B data libraries. Two methods of calculating the energy contribution from radiative capture were proposed since this quantity is reactor specific. Both methods used MCNP5; however, a heating tally was used in the first method and the capture reaction rate tally was used in the second method. The fission Q-value of SAFARI-1 was calculated successfully using these methods. Using MCNP5 and the Q-value, 201.20 MeV/fission was obtained and using the ENDF/B-VII library, 200.30 MeV/fission was obtained. The final Q-value calculated was average of the two methods with an associated standard error to add to the credibility of the results. The final Q-value result was 200.8 MeV/fission ± 0.6 MeV/fission. This result compared well with literature given in Chapter 2. There is confidence in the result, as the entire SAFARI-1 core together with the water surrounding the core was modelled. If there were any neutron or gamma radiation leakages from the core, they were accounted for.

In Section 4.4, we showed that the Q-value can be calculated at any stage in a typical reactor cycle. The Q-value was calculated three days into the cycle using MCNP5 and obtained 201.2 MeV/fission. Calculating the Q-value at the EOC resulted in 200.8 MeV/fission. We see that the difference is not significant, and therefore conclude that fuel burn-up does not affect the Q-value.

Lastly, the spatial heat distribution was successfully calculated for SAFARI-1. A total heating of 19.98 MW was obtained. This result is consistent with the operating power of the reactor, which is 20 MW. It was found that 97% of the heat produced from fission in SAFARI-1 is deposited within the fuel and 3% to the surrounding parts of the reactor core.

5.1 Future Work

Currently, the data libraries used in MCNP does not contain information about decay energies from capture. Beta decay deposits its energy locally, and other codes such as FISPACT can be used to calculate it. A problem arises with gamma decay energy deposition. Gamma rays are transported in the system, and therefore requires an MCNP calculation. In order to include the gamma decay energy deposition in the system, future work will focus on including these energies in the data libraries that MCNP uses. Secondly, future work will also focus on using newer versions of MCNP, such as MCNP6.2 [21] to calculate the Q-value.

REFERENCES

- [1] M. Dupont E. Soppera, N. Bossant. Nuclear data sheets, volume 120, janis 4: An improved version of the nea java-based nuclear data information system, June 2014.
- [2] R.J. Lamarsh. Introduction to Nuclear Reactor Theory. Addison-Wesley Publishing Company, 2 edition, September 1972.
- [3] K. S. Krane. *Introductory Nuclear Physics*. Oregon State University, 1995.
- [4] X-5 Monte Carlo Team. *MCNP- A General Monte Carlo N-Particle Transport Code, Version 5*. Los Alamos National Laboratory, volume 1 edition, April 2003. Revised 02/01/2008.
- [5] J. Peterson and G. Ilas. Calculation of heating values for the high flux isotope reactor. In *PHYSOR 2012 – Advances in Reactor Physics – Linking Research, Industry, and Education*, pages 1–10, Knoxville, Tennessee, USA, April 15–20 2012. American Nuclear Society.
- [6] J. W. Sterbentz. Q-value (mev/fission) determination for the advanced test reactor. Technical Report Revision 0, Idaho National Laboratory, Idaho Falls, Idaho 83415, October 2013.
- [7] G. Yesilyurt. Coupled nuclear-thermal-hydraulic calculations for vthrs. *Transactions of American Nuclear Society*, 102(1):519 – 521, 2010.

- [8] F.B. Brown. Monte carlo advances and challenges. la-ur-08-05891. In *PHYSOR Conference*, Interlaken, Switzerland, 14-19 September 2008.
- [9] A.K. Prinja and E.W. Larsen. *General Principles of Neutron Transport.*, volume I. Springer, Boston, MA, 2010.
- [10] J.J. Duderstadt and L.J. Hamilton. *Nuclear Reactor Analysis*. John Wiley & sons Inc., 1942.
- [11] Prinsloo. Oscar-4 system overview, rrt-oscar-rep-12002. Technical report, Necsca, 2012.
- [12] E. Hussein. *Monte Carlo Particle Transport with the MCNP Code*. URL <https://canteach.candu.org/Content%20Library/20043514.pdf>.
- [13] L.L. Schwarz A. Schwarz, R. Carter. *Modification to the Monte Carlo N-Particle (MCNP) Visual Editor (MCNPVised) to Read in Computer Aided Design (CAD) Files*.
- [14] O. M. Zamonsky. Deposition of energy due to fission product decay in safari-1 using mcnp5, rrt-safa-rep-17013. Technical report, Necsca, June 2017.
- [15] M.B. Chadwick et al. Endf/b-vii.0 nuclear data for science and technology: Cross sections, covariances, fission product yields and decay data. *Nuclear Data Sheets*, 112(12):2887 – 2996, 2011. ISSN 0090-3752. doi: <https://doi.org/10.1016/j.nds.2011.11.002>. URL <http://www.sciencedirect.com/science/article/pii/S009037521100113X>. Special Issue on ENDF/B-VII.1 Library.
- [16] M.B. Chadwick et al. Endf/b-vii. 1 nuclear data for science and technology:

Cross sections, covariances, fission product yields and decay data. *Nuclear Data Sheets*, 112(12):2887–2996, 2011.

- [17] K.E. Holbert. Atomic number density. December 2014.
<http://holbert.faculty.asu.edu/eee460/NumberDensity.pdf>.
- [18] R.A. Forrest. *FISPACT-2007: User manual*. EURATOM/UKAEA Fusion Association, i edition, February 2007.
- [19] X-5 Monte Carlo Team. *Handbook of Nuclear Engineering: Vol.1: Nuclear Engineering Fundamentals*, 2010.
- [20] Endf database general statistics, 02 2018. URL
http://www.nndc.bnl.gov/exfor/x4stat/endl_stat.htm.
- [21] Monte Carlo Team. *MCNP, LA-UR-17-29981: MCNP User's Manual Code Version 6.2*.

APPENDIX A

MCNP: EXPLANATION OF INPUT AND OUTPUT

A.1 MCNP Input

Below is a section taken from an input used to calculate the heat produced in the core box. Next to each line of the input below, there is an explanation.

PROBLEM DATA CARDS *****

MODE N P - The mode is the radiation particle that is being transported: in this case, it is neutrons and photons.

kcode 200000 1.000 100 1000 - Kcode is a card in MCNP that defines the number of source histories (200 000), the criticality ($K_{\text{eff}} = 1$), the number of inactive cycles (100) and the number of active cycles (1000).

prdmp 1100 1100 0 2 - The print and dump cycle card in MCNP is used to define the increments of printing tallies and dumping to the RUNTPE file.

PIKMT 92234.70 1 18001 1 92235.70 1

18001 1 92236.70 1 18001 1 92238.70 1

18001 1 92237.70 1 18001 1 93237.70 1

18001 1 94239.70 1 18001 1 94240.70 1

18001 1 94241.70 1 18001 1 - The PIKMT card is the photon bias card that was used in the spatial heat calculation. The ZA (atomic and mass numbers) identification (ZAID) number of the material producing prompt gammas is placed with the PIKMT card. The ZAID number comprises of the atomic number, mass number and cross-section identifier of the element or nuclide. This can be taken from the MCNP manual.

print 30 32 120 130 - The print card indicates which tables the user wants to print in the output. The table numbers can also be found in the MCNP manual.

c ----- TALLIES ----- c

fc16 Heating - N - MeV - The F6 tally number 1 in MeV units.

f16:n 7001 7002 7004 - The mode of transport is the neutrons and cell numbers of the core box: the mode can also be photons, in which case the tally will become f06:p

c - comment line

fc16 Heating - N - MeV

f16:n 7001 7002 7004

sd16 1 1 1 - The SD card contains the number of cell entries divided by 1

A.2 MCNP Output

Based on the information in Appendix A.1, the corresponding section of the output file is given below with explanations.

1tally 16 - In the results section of the output, the first line gives the tally type, which is F6 and the tally number, which is 1.

nps = 20005744 - nps is the number of histories that were run for each cycle.

Heating - N - MeV tally type 6 track length estimate of heating. units
mev - This line is the description of the tally. I.e. heating tally type 6 for F6
and units of results in Mev.

tally for neutrons number of histories used for normalizing tallies =
16000000.00

masses cell: 7001 7002 7004

1.00000E+00 1.00000E+00 1.00000E+00 - the cell masses are usually printed
here: however, since the SD=1, the mass is 1.

cell 7001 5.34284E-04 0.0035

cell 7002 9.74037E-04 0.0027

cell 7004 1.05325E-03 0.0027 - These are the heating results obtained in
MeV with the associated standard error.

Each tally result will output a table with statistical checks so that the user can
determine the reliability of the results. Below is an example of the checks taken
from the same output above.

If all 10 statistical checks are passed in Fig. A.1, it is a good indication that the results of the tally converged and we can have confidence in the results. This work did not focus on statistical analysis in MCNP: however, the MCNP manual explains the statistics in detail.

```

results of 10 statistical checks for the estimated answer for the tally fluctuation chart (tfc) bin of tally 16
-----relative error-----
value  decrease  decrease rate
<0.10  yes         1/sqrt(nps)
0.00   yes         yes
yes    yes         yes

-----variance of the variance-----
value  decrease  decrease rate
<0.10  yes         1/nps
0.00   yes         yes
yes    yes         yes

--figure of merit--
value  behavior
constant  random
constant  random
yes       yes

--pdf-slope
>3.00
4.01
yes

```

Figure A.1: Example of statistics check from MCNP output